OXFORD

Cerebral Cortex, 2023, **33**, 2734–2747
https://doi.org/10.1093/cercor/bhac238
Advance access publication date 11 June 2022
Original Article

Neural representations of competing stimuli along the dorsal and ventral visual pathways during binocular rivalry

Ce Mo[1,†], Junshi Lu[2,3,†], Chao Shi[2,3], Fang Fang[2,3,4,*]

[1]Department of Psychology, Sun Yat-Sen University, Guangzhou 510006, Guangdong, China,
[2]School of Psychological and Cognitive Sciences and Beijing Key Laboratory of Behavior and Mental Health, Peking University, Beijing 100087, China,
[3]IDG/McGovern Institute for Brain Research, Peking University, Beijing 100087, China,
[4]Peking-Tsinghua Center for Life Sciences, Peking University, Beijing 100087, China

*Corresponding author: School of Psychological and Cognitive Sciences, Peking University, 52 Haidian Road, Beijing, 100087, China. Email: ffang@pku.edu.cn
https://www.psy.pku.edu.cn/english/people/faculty/professor/fangfang/index.htm

†Ce Mo and Junshi Lu contributed equally to this work.

Binocular rivalry arises when two discrepant stimuli are simultaneously presented to different eyes, during which observers consciously experience vivid perceptual alternations without physical changes in visual inputs. Neural dynamics tracking such perceptual alternations have been identified at both early and late visual areas, leading to the fundamental debate concerning the primary neural substrate underlying binocular rivalry. One promising hypothesis that might reconcile these seemingly paradoxical findings is a gradual shift from interocular competition between monocular neurons to pattern competition among binocular neurons. Here, we examined this hypothesis by investigating how neural representations of rivalrous stimuli evolved along the visual pathway. We found that representations of the dominant and the suppressed stimuli initially co-existed in V1, which were enhanced and attenuated respectively in extrastriate visual areas. Notably, neural activity in V4 was dictated by the representation of the dominant stimulus, while the representation of the suppressed stimulus was only partially inhibited in dorsal areas V3A and MT+. Our findings revealed a progressive transition from the co-existing representations of the rivalrous inputs to the dictatorial representation of the dominant stimulus in the ventral pathway, and advocated different cortical evolutionary patterns of visual representations between the dorsal and the ventral pathways.

Key words: binocular rivalry; inverted encoding model; progressive transition; co-existing representation; dictatorial representation.

Introduction

When discrepant visual images are presented to different eyes, they alternate in perceptual dominance every few seconds, during which one image becomes visible and the other vanishes from visual awareness (Blake and Logothetis 2002; Alais and Blake 2005). This remarkable phenomenon is known as binocular rivalry. Because a fundamental hallmark of binocular rivalry is the intriguing dissociation between constant physical stimulation and fluctuating perceptual experience (Clifford 2009), understanding its neural correlates therefore enables a giant leap in the quest for revelation of the mystery of consciousness (Zhang et al. 2011; Blake et al. 2014).

Despite extensive research efforts, our knowledge of the neural correlates of binocular rivalry is nonetheless clouded by previous inconclusive findings (Blake 2001; Tong 2001). On one hand, pioneering single-unit recording studies have shown that the neuronal activity enhancement corresponding to the dominant percept during binocular rivalry is more pronounced in higher-order visual areas (Logothetis et al. 1996; Tong et al. 1998). The percentage of neurons modulated by the alternating percepts during binocular rivalry increased from approximately 40% in MT (Logothetis and Schall 1989) and V4 (Leopold and Logothetis 1996) to 90% in inferotemporal cortex and superior temporal sulcus (Sheinberg and Logothetis 1997). Meanwhile, only a small portion (~20%) of V1/V2 neurons exhibited such percept-related changes in firing rate. These findings suggest that binocular rivalry is mainly mediated by the competition between binocular neurons representing the two dichotomous image patterns in higher order visual areas (i.e. pattern competition). On the other hand, tight coupling between fMRI signal and observers' percept was found in V1 (Polonsky et al. 2000; Lee et al. 2005, 2007) and lateral geniculate nucleus (Haynes et al. 2005; Wunderlich et al. 2005). Tong and Engel (Tong and Engel 2001) investigated the dynamics of V1 activation during binocular rivalry between two orthogonal gratings, one of which was presented at the monocular blind-spot of the right eye. They found that the V1 activation representing the blind-spot grating closely tracked its perceptual

Received: January 26, 2022. **Revised:** May 7, 2022. **Accepted:** May 8, 2022

dominance fluctuation, suggesting that binocular rivalry involves competition between monocular neurons before the convergence of the two eye's inputs (i.e. interocular competition). The two lines of evidence have in turn fueled the hybrid theory that binocular rivalry does not arise solely at the early or the late stage of visual processing, but rather from a cascade of competitive interactions across multiple levels of the visual hierarchy (Watson et al. 2004; Pearson and Clifford 2005; Tong et al. 2006). However, the hybrid theory does not make a clear prediction concerning how the representations of the rivalrous monocular inputs evolve from lower to higher visual areas.

In light of these previous research works, we proposed that the seemingly paradoxical findings might be reconciled by a progressive transition from the co-existing representations of the dichotomous monocular stimuli to the dictatorial representation of the dominant stimulus (i.e. the progressive transition hypothesis). Initially, the two monocular images are encoded by sparsely distributed, feature-selective neurons in early visual areas, forming a veridical, information-rich representation of each eye's input despite their perceptual incompatibility. As the two monocular images compete for perceptual dominance, the neural representation of the suppressed eye's input gradually recedes and eventually gives way to the representation of the dominant eye's input as a result of increasing inhibitory interactions along the visual pathway. Unfortunately, however, examination of the progressive transition hypothesis is complicated by the difficulty of interrogating the representational contents of visual cortex via conventional neurophysiological or BOLD measurements. While the limited spatial coverage of single unit recordings might result in inadequate sampling of the sparse, feature-selective neurons, conventional univariate analyses of BOLD signals were oblivious to the representational contents of these neuronal populations (Haynes and Rees 2005; Kamitani and Tong 2005; Haynes and Rees 2006). Furthermore, comprehensive inter-cortical comparison of the neural dynamics associated with binocular rivalry is highly challenging with only one feature type, because different cortical regions drastically vary in their respective neuronal tuning properties to different types of stimuli. A typical example is the functional division of labor between the dorsal and the ventral visual pathway in which dorsal areas are specialized for processing visual motion whereas ventral areas are optimally engaged in processing shape and object information (Mishkin et al. 1983; DiCarlo et al. 2012).

Here, using fMRI-based inverted encoding model (IEM) analysis (Brouwer and Heeger 2009, 2013; Sprague and Serences 2013; Ester et al. 2015; Sprague et al. 2016), we investigated neural representations of the two incompatible monocular stimuli in multiple visual areas (V1-V3, V3A, MT+, and V4). To provide a more comprehensive assessment of how representations of the dominant and the suppressed stimuli might interact in different areas, we used two of the most representative visual features with clear and well-defined neuronal tunings, namely orientation and motion direction, as our test bed. Subjects were presented with two orthogonal gratings or random dot fields moving in opposite directions in different eyes, thus leading to two rivalrous orientations or motion directions (i.e. the rivalry condition). Benefitting from the IEM's ability to interrogate the feature-specific information encoded in the population activities (Sprague et al. 2018; Mo et al. 2019; Rademaker et al. 2019), we were able to track how the representations of the rivalrous features were modulated in different visual areas. To evaluate the rivalry effects, we also included a duration-matched perceptual replay condition in which subjects experienced alternating physical stimulation that mirrored perceptual alternation in the rivalry condition. We found that the representations of the rivalrous stimuli (orientation and motion direction) were jointly hosted in V1. Furthermore, we identified a progressive transition from the co-existing representations of the rivalrous stimuli to the dictatorial representation of the dominant stimulus along the ventral visual pathway, with neural activity in V4 completely dictated by the dominant stimulus. Notably, despite a similar transition along the dorsal visual pathway, such a dictatorial representation of the dominant stimulus was not found in the dorsal areas V3A and MT+, which are situated at the same and an even higher level in the visual processing hierarchy with respect to V4.

Methods

Subjects

A total of nineteen subjects (ten females, 18–26 years old) participated in the study. Each rivalry experiment (orientation rivalry and motion direction rivalry) involved ten subjects, with one subject participating in both experiments. All subjects had normal or corrected-to-normal vision and reported no known neurological or visual disorders. Written informed consent was collected for each subject prior to the study. Before the fMRI scanning sessions, all subjects were screened for difficulty in fusing monocular stimuli in a pilot behavioral study. The experimental protocols were approved by the human subject review committee at Peking University.

Stimuli and task

Experimental stimuli were generated using the Psychophysics Toolbox 3(Kleiner et al. 2007). In the orientation rivalry experiment, stimuli in the rivalry condition consisted of two annular sinusoidal gratings that were presented to different eyes (inner radius: 0.5°; outer radius: 3.5°; spatial frequency: 0.5 cycles/°; Michelson contrast: 0.66; mean luminance: 30.2 cd/m^2). The contrast of the gratings was reversed every 0.5 seconds. For each subject, the orientations of the two gratings were randomly chosen from three possible orthogonal pairs (15°–105°, 45°–135°, and 75°–165°). Subjects were

required to report their perceptual experience using one of three buttons that corresponded to the left-eye grating, the right-eye grating, and a piecemeal blend of the two gratings (i.e. transition), respectively. In the replay condition, we simulated the perceptual alternation during binocular rivalry (Knapen et al. 2011). Specifically, for the periods of reported perceptual dominance, the dominant grating was presented to the corresponding eye, with a uniform blank background presented to the other eye. For the periods of transition (i.e. blended percept), the previously dominant grating was presented to both eyes, whose orientation smoothly switched to the orientation of the previously suppressed grating by means of a straight boundary sweeping across the grating from a randomly selected side, thus replacing the previously dominant grating with the previously suppressed one. In addition, transient transitions (< 1 s) were replayed by the decrease in transparency of one grating and the simultaneous increase in transparency of the other. The combination of the two stimulus presentation schemes thus created the perception of orientation that alternated in the same temporal sequence of perceived orientation as reported in the rivalry condition. Subjects, unaware of the differences between the rivalry and replay conditions, performed the same task as in the rivalry condition.

The task and the stimulus presentation schemes in the motion direction rivalry experiment were similar to those in the orientation rivalry experiment. The rivalrous stimuli consisted of two monocular random dot kinematograms (RDKs) moving in opposite directions. Each RDK contained 200 visible dots within an annular aperture (inner radius = 0.5°; outer radius = 3.5°; speed: 6°/s; diameter: 0.12°; luminance: 1.22 cd/m^2). All dots in a RDK moved in the same direction and had a lifetime of 350 ms. Similarly, the directions of the two RDKs were chosen randomly from four possible pairs (22.5°–202.5°, 67.5°–247.5°, 112.5°–292.5°, and 157.5°–337.5°) for each subject. To simulate the perceptual transitions during the motion direction rivalry in the replay condition, the proportion of dots moving in the previously dominant direction linearly decreased, which was accompanied by the simultaneous increase in the proportion of dots moving in the opposite direction from 0% to 100%. In both experiments, the background was uniformly gray with its luminance set to the mean luminance of the sinusoidal gratings (30.2 cd/m^2). A black square-shaped box (size: 5°) that framed the grating stimulus and a crosshair fixation were presented to both eyes to aid the fusion of the monocular stimuli.

fMRI experiments

Stimuli were presented on a rear-projection screen with an MRI-compatible projector (resolution: 1,024 × 768, fresh rate: 60 Hz) in the scanner room. Subjects viewed the stimuli through a mirror mounted on the head coil from a viewing distance of 60 cm. The two monocular stimuli were presented on the left and right halves of the screen. Dichoptic projection in the scanner was achieved by adjusting the viewing angle from which light enters each eye using a pair of prisms. A customized septum mounted on the head coil was used to block the crosstalk between the two eyes (Schurger 2009). In both the orientation and the motion rivalry experiments, each subject completed six fMRI sessions, including a localizer session for retinotopic mapping and regions of interest (ROI) definition, a model training session for IEM parameter estimation, and four main sessions.

In the localizer session, retinotopic visual areas (V1, V2, V3, V3A, and V4) were identified for both experiments using a standard phase-encoded method. Subjects viewed a continuously rotating wedge or an expanding ring that created traveling waves of neural activity in visual cortex. We delineated the horizontal and vertical meridians of the visual field using the waves projected onto gray- and white-matter boundary surface reconstructions for each hemisphere. Using these meridians, we defined the areas V1, V2v, V2d, V3v, V3d, hV4, and V3A. In each visual area, the ROI corresponding to the stimulus aperture was defined as the cortical voxels that responded more strongly to a flickering checkerboard that subtended the stimulus aperture than to the blank screen ($P < 0.01$, uncorrected). Additionally, for the motion rivalry experiment, ROI in MT+ was defined as the cortical voxels that responded more strongly to the moving dots than to the stationary dots inside the stimulus aperture ($P < 0.01$, uncorrected) within or near the occipital continuation of the inferior temporal sulcus. Parameters of the dot stimuli were identical to those in the motion rivalry experiment, except that each dot moved in a random direction. Unless otherwise indicated, data were pooled across hemispheres and across the dorsal and ventral parts of each respective visual area.

The model training session in both the orientation and the motion rivalry experiments involved eight functional runs. Subjects viewed two identical gratings or RDKs that were presented to both eyes when they performed a color change detection task at fixation. In the orientation rivalry experiment, the gratings had one of six possible orientations (from 15° to 165° in steps of 30°). Each run consisted of twelve 12-s stimulus blocks, interleaved with thirteen fixation blocks of 12 s. Each orientation was presented in two blocks and the order of the six orientations was randomized. In the motion rivalry experiment, the RDKs had one of eight possible directions (from 22.5° to 337.5° in steps of 45°). Each run consisted of sixteen 12-s blocks, interleaved with seventeen 12-s fixation blocks. The parameters of the gratings and the RDKs were the same as those in the main sessions as described previously.

Each main session in both experiments involved six rivalry runs and six replay runs in an interleaved order and always started with a rivalry run. In a rivalry run, the rivalrous stimuli (gratings or RDKs) were presented to the two eyes for 90 seconds after an initial fixation period of 20 s. The offset of the rivalrous stimuli was immediately

followed by another fixation period of 20 s. Each rivalry run was followed by a replay run. The temporal structure of the replay run was identical to that of the rivalry run, which was comprised of an initial 20-s fixation period, a 90-s stimulus presentation period and a final 20-s fixation period. Notably, the rivalrous stimuli were replaced by the stimuli that mimicked subjects' perceptual alternation in the preceding rivalry run. Throughout all scanning sessions, subjects were required to fixate at the central fixation cross and refrain from any possible eye movement.

MRI data acquisition

MRI data was collected on a 3 T Siemens Prisma MRI scanner with a 20-channel head coil at the Center for MRI Research at Peking University. Functional images were acquired with Multiband EPI sequence (TR: 1,000 ms; TE: 30 ms; flip angle: 90°). Twenty-eight slices covering the occipital lobe and parts of the temporal and parietal lobes (slice thickness: 3 mm; FOV: 212×212 mm^2; in-plane resolution: 2×2 mm; no gap) were oriented roughly perpendicular to the calcarine fissure, with the most posterior slice positioned near the occipital pole. Anatomical images were acquired with a T1-weighted MP-RAGE sequence (TR: 2,530 ms; TE: 2.98 ms; resolution: $1 \times 1 \times 1$ mm^3) at the beginning of each scanning session.

MRI data analyses

Functional data were processed using SPM8. The preprocessing procedure included head motion correction, linear trend removal and high-pass (0.015 Hz) filtering. For each subject, the preprocessed functional volumes in each scanning session were first aligned to the anatomical volume in that session and then were co-registered to the anatomical volume acquired in the localizer session. The anatomical volume in the localizer session thus served as a common anatomical template, which was segmented and inflated to reconstruct the cortical surface using FreeSurfer. A standard general linear modeling (GLM) procedure was employed to estimate the BOLD response amplitudes of each voxel in each condition. Specifically, a box-car function was defined for each stimulus block for the model training session data, while a box-car function was defined for each reported percept (left-eye stimulus, right-eye stimulus and piecemeal blend) for the main session data. These box-car functions were convolved with a canonical hemodynamic response function to generate the regressors in the corresponding design matrix. The voxel-wise BOLD responses (i.e. beta values) obtained from the GLM procedure were z-transformed across all voxels in each ROI and were used for subsequent analyses.

According to the assumption of IEM (Sprague and Serences 2013; Ester et al. 2015; Sprague et al. 2016; Sprague et al. 2018; Rademaker et al. 2019), the BOLD response to a feature stimulus (i.e. orientation or motion direction) in a brain region could be expressed as a weighted linear sum of the responses of multiple feature-selective channels:

$$\boldsymbol{B} = \boldsymbol{WC}$$

where $\boldsymbol{B}$ is the matrix of voxel-wise BOLD responses in different blocks (model training runs) or time periods (main runs) (m voxels-by-n blocks/time periods), $\boldsymbol{W}$ is the matrix of linear weights for these feature-selective channels (m voxels-by-k channels) that mapped the channel outputs to the BOLD signals, and $\boldsymbol{C}$ is the matrix of channel responses in each block or time period (k channels-by-n blocks/time periods). The IEM analysis thus proceeded in two stages: First, the channel weights (i.e. $\boldsymbol{W}$) were estimated based on the data in the model training session. To this end, we modeled the idealized tuning of the orientation channels as the half-wave rectified sinusoidal functions centered at 15° to 165° in steps of 30° that were raised to the 5th power. For the motion direction channels, the idealized tuning functions were modeled in a similar manner, except that they were centered at 122.5° to 337.5° in steps of 45° and were raised to the 7th power. These functions constituted a steerable filter similar to the neuronal tuning curves in visual areas (Ester et al. 2015; Rademaker et al. 2019). Hence, for each stimulus block in the model training runs, the channel responses could be predicted from these idealized tuning functions. For each ROI, the weight matrix $\boldsymbol{W}$ could thus be estimated based on the predicted channel responses using ordinary least-square (OLS) regression:

$$\hat{\boldsymbol{W}} = \boldsymbol{B_1}\boldsymbol{C_1}'\left(\boldsymbol{C_1}\boldsymbol{C_1}'\right)^{-1}$$

where each row in $\boldsymbol{B_1}$ corresponds to a voxel in the ROI and each column corresponds to a stimulus block (96 and 128 blocks in the model training session for the orientation and the motion rivalry experiment, respectively). $\boldsymbol{C_1}$ contains the predicted channel responses for the presented stimulus in each stimulus block.

Second, the estimated weight matrix was applied to the data from the rivalry runs and the replay runs respectively, which reconstructed the channel responses during binocular rivalry and perceptual replay:

$$\boldsymbol{C_2} = \left(\hat{\boldsymbol{W}}'\hat{\boldsymbol{W}}\right)^{-1}\hat{\boldsymbol{W}}'\boldsymbol{B_2}$$

where $\boldsymbol{B_2}$ is the matrix of voxel-wise BOLD responses in the ROI when an orientation or motion direction was perceived (during binocular rivalry) or presented (during perceptual replay). $\boldsymbol{C_2}$ is the matrix comprised of column vectors of reconstructed channel responses in each perceptual dominance period or stimulus replay period. For the rivalry runs, the reconstructed channel responses in each dominance period were circularly shifted to align the corresponding dominant orientation or motion direction in that period to a common 0° center (re-centering). Hence, the re-centered channel responses could be averaged across different

dominance periods to obtain the channel response profile. In the channel response profile, 0° denoted the dominant orientation or motion direction, while ±90° and ± 180° denoted the suppressed orientation and motion direction, respectively. For the replay runs, the reconstructed channel responses were re-centered to the presented orientation or motion direction and averaged. In the resultant channel response profile, 0° hence denoted the presented orientation or motion direction. To quantify the representational advantage of the dominant stimulus in the orientation rivalry experiment, we first calculated the response difference between the 0° and the ±90° channels for the rivalry and the replay condition, respectively. We then divided the response difference in the rivalry condition by that in the replay condition to obtain the suppression index. Suppression index of the motion direction rivalry experiment was computed in a similar manner, except that the channel response difference between the 0° and the ±180° channels was used for the computation.

Results

Orientation rivalry

According to the hypothesis of IEM, the measured BOLD signal to an orientation in each voxel could be decomposed into the weighted responses of a series of information channels that modeled the orientation-selective neuronal populations with different preferences. To implement the IEM, the orientation rivalry experiment proceeded in three stages. First, we delineated the regions of interest (ROIs) in retinotopic visual areas (V1-V4 and V3A) in the functional localizer session. Second, we estimated the respective contributions (i.e. weights) of these information channels to the voxel-wise BOLD responses for each ROI in an independent model training session (Fig. 1A). Finally, the estimated weights were applied to the BOLD signals recorded in the main sessions to reconstruct the channel responses when subjects perceived one of the alternating orientations during binocular rivalry or perceptual replay (Fig. 1B). In the main sessions, the gratings filled an annular aperture centered at the fixation cross. Subjects were instructed to maintain fixation and respond with a key press that corresponded to the left-eye orientation, the right-eye orientation or a blend of the two orientations when viewing two orthogonal gratings through different eyes.

Behavioral data showed that, for both the left-eye and the right-eye orientations, the distributions of dominance durations could be well characterized by a gamma distribution (Fig. 2A). For each subject, we fitted a gamma probability density function to each eye's dominance duration distribution and performed a Kolmogorov–Smirnov test to assess the goodness of fit. Next, we verified that there was no difference in dominance duration between the two eyes (mean duration of left-eye orientation: 3.32 s, mean duration of right-eye orientation: 3.35 s, Wilcoxon's signed rank test: $P = 0.79$) by comparing the mean of the fitted distribution across the subjects. We then reconstructed the orientation channel responses in either dominance period (left-eye orientation or right-eye orientation) in the rivalry runs in each ROI based on the fMRI data. The reconstructed channel responses were circularly shifted to align the perceptually dominant orientation in each dominance period to a common 0° center (i.e. re-centering). It is important to note that re-centering did not alter the numerical relationship between the channel responses. After re-centering, 0° and ± 90° corresponded to the dominant and the suppressed orientations, respectively. The re-centered channel responses were then averaged across all runs to obtain the channel response profile for the rivalry condition. The same procedure was employed to obtain the channel response profile for the replay condition in which 0° corresponded to the orientation viewed by the subjects in either dominance period and ± 90° corresponded to the orientation orthogonal to the viewed grating. Notably, because the orthogonal orientation was not presented to the subjects during replay, the ±90° channel response in the replay condition was therefore used as the baseline against which we tested for the representation of the physically presented or perceptually dominant orientation.

We first validated the IEM approach by examining whether information of the presented orientation in the replay condition and of the perceived orientation in the rivalry condition could be reliably recovered from BOLD signal patterns in the ROIs. For the replay condition, we found that the channel response functions in all ROIs consistently exhibited a symmetrical, uni-modal profile, with a clear peak at 0° (i.e. the presented orientation) that was significantly stronger than the baseline (Fig. 3, red curves, paired-t test, V1: $t_{(9)} = 10.296$, V2: $t_{(9)} = 9.578$, V3: $t_{(9)} = 14.558$, V4: $t_{(9)} = 8.247$, V3A: $t_{(9)} = 17.331$, all $ps < 0.001$). Moreover, for the rivalry condition, responses of the 0° channel (i.e. the dominant orientation) were also significantly stronger than the baseline in all ROIs (Fig. 3, blue curves, paired-t test: V1: $t_{(9)} = 8.393$, V2: $t_{(9)} = 8.935$, V3: $t_{(9)} = 7.819$, V3A: $t_{(9)} = 9.310$, V4: $t_{(9)} = 7.505$, all $ps < 0.001$). Together, these findings showed that orientation-specific information of both the viewed grating during perceptual replay and the perceived grating during binocular rivalry could be robustly read out via the channel response functions obtained by the IEM.

Having established the validity of our approach, we examined the first part of our progressive transition hypothesis, namely the co-existing and competing representations of the two eye's inputs. We reasoned that if the suppressed orientation was represented at the initial stage of visual cortical processing as predicted by the progressive transition hypothesis, then one would expect a stronger channel response corresponding to the suppressed orientation in comparison to the baseline in V1. Otherwise, there should be no difference. We found that, in V1, the ±90° channel response (i.e. the suppressed

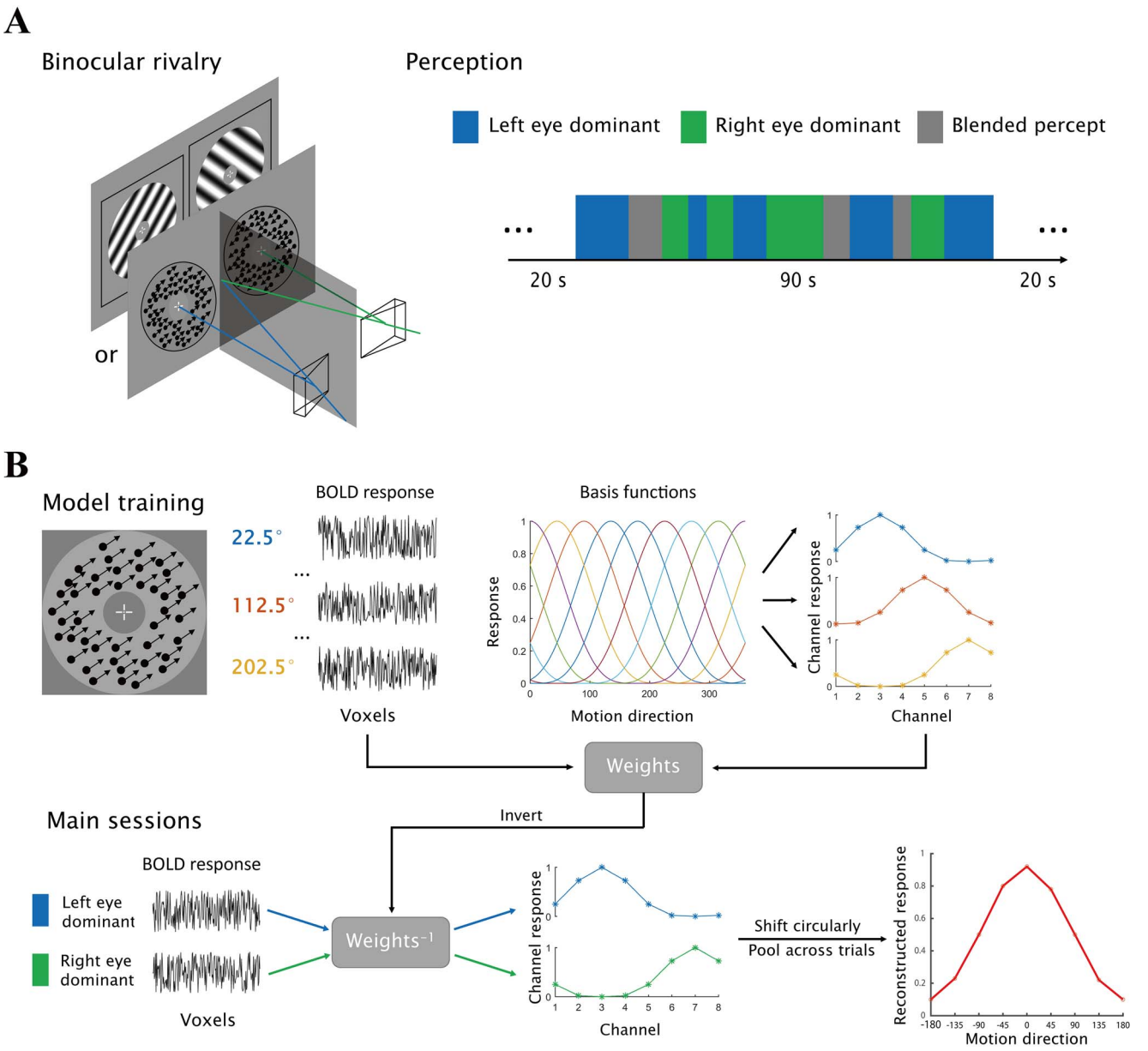

Fig. 1. Representation reconstruction procedure for binocular competing features. **A)** Binocular rivalry experiment. Subjects viewed two orthogonal orientations or two RDKs moving in opposite directions through different eyes and experienced one of three possible perceptual states (left-eye stimulus dominant, right-eye stimulus dominant and the blended percept) shown in different colors. **B)** Pipeline of the IEM analysis. In the model training sessions (for better illustration, only the motion direction rivalry experiment procedure is elaborated here), subjects were presented with an RDK moving in one of eight possible directions that corresponded to the respective preferred direction of eight motion channels. The idealized tuning of these channels was characterized as smooth, Gaussian-like basis functions (shown in different colors), based on which the predicted channel responses to each presented RDK were obtained. Channel weights were estimated from the multi-voxel BOLD response pattern extracted from each ROI and the predicted channel responses for each presented motion direction. Multi-voxel BOLD response patterns corresponding to each dominance period in the main sessions were extracted and multiplied by the inverted channel weights to obtain the channel response profiles. These channel response profiles were then circularly shifted to align the 0° channel to the dominant direction. In the orientation rivalry experiment, a sinusoidal grating of one of six orientations was presented in the model training sessions and two orthogonal gratings were presented in the main sessions.

orientation) was stronger than the baseline (paired-t test: $t_{(9)} = 2.817$, $P = 0.02$), and was weaker than the 0° channel response (i.e. the dominant orientation) ($t_{(9)} = 5.633$, $P = 0.002$). This result provided clear demonstration that the representation of the suppressed eye's input, albeit weaker in strength, was also hosted in V1 alongside the representation of the dominant eye's input (Fig. 3A). Moreover, this result also extended previous neurophysiological findings by showing that the competitive advantage of the dominant over the suppressed orientation was reflected not only in activities of single neurons, but also in the population-level activity patterns in primary visual cortex. Together, our findings indicated that the input information from the suppressed eye was not immediately discarded after it reached V1, but was retained in the corresponding neurons that engaged in competitive interaction with those encoding the dominant eye's input (i.e. interocular rivalry).

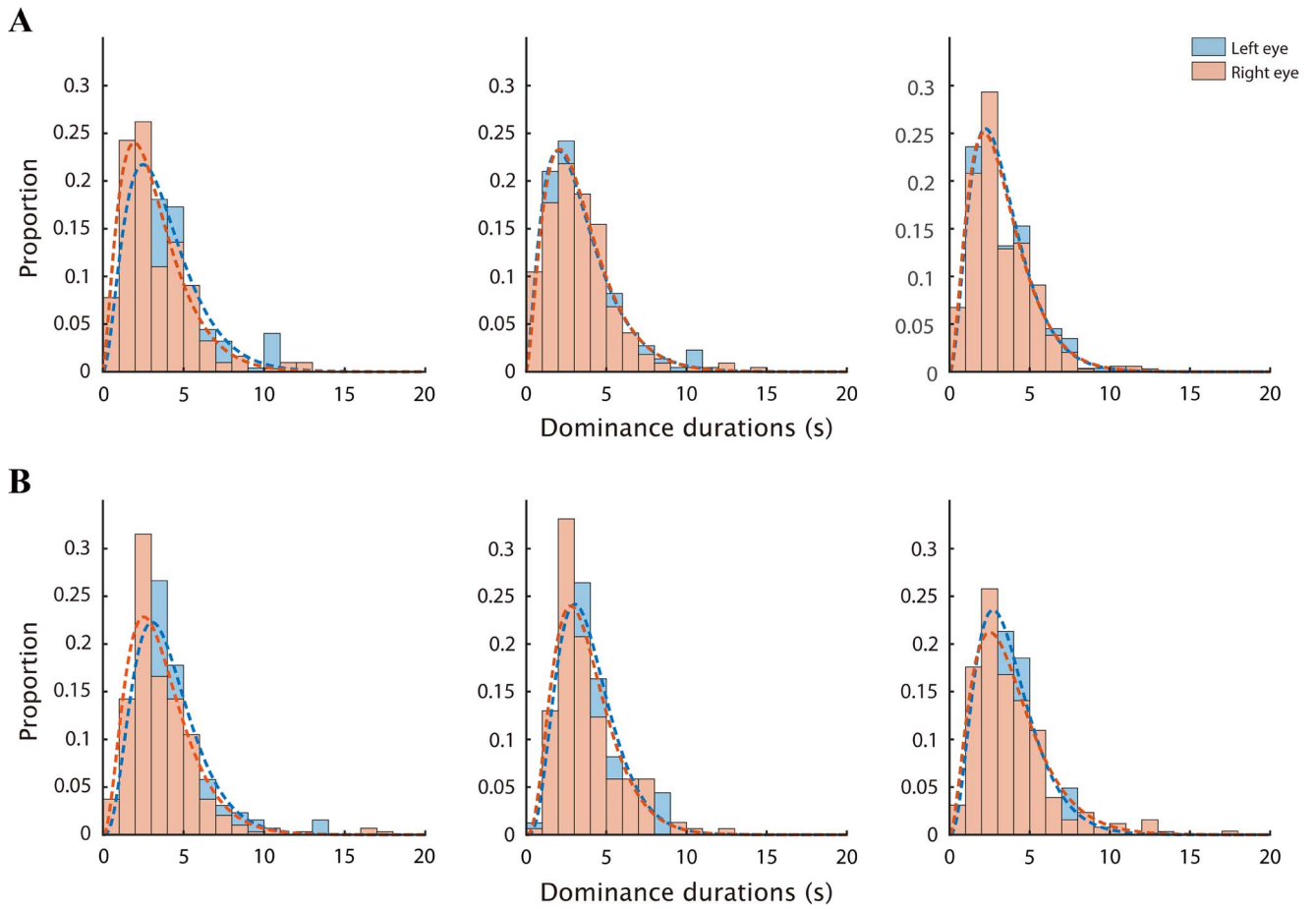

Fig. 2. Eye-specific dominance duration distributions of three representative subjects in **A)** the orientation rivalry experiment and **B**) the motion direction rivalry experiment. Dashed curves denote the fitted gamma probability density functions. Data that yielded the lowest, the intermediate and the highest goodness of fit among all subjects are shown from left to right, respectively.

The second part of our hypothesis concerns a progressive transition from the co-existing representations of the two eye's inputs to the dictatorial representation of the dominant stimulus, according to which one would expect increasing representational advantage of the dominant over the suppressed orientation along the visual pathway. To test this idea, we proceeded to investigate the representations of the dominant and the suppressed orientations during binocular rivalry in visual areas beyond V1. Similarly, stronger representations of the dominant orientation in comparison to the suppressed orientation were found in extrastriate visual areas (paired-t test, V2: $t_{(9)} = 9.663$, V3: $t_{(9)} = 10.736$, V4: $t_{(9)} = 17.527$, V3A: $t_{(9)} = 11.628$, all $ps < 0.01$), suggesting that the modulation effect of binocular rivalry was not limited to V1, but persisted in the downstream visual areas. However, a close scrutiny revealed that the difference between the dominant and the suppressed orientation representations was not invariant across extrastriate visual areas. Specifically, while there was a salient distinction between the channel response profiles for the rivalry and the replay conditions in V1, they became increasingly similar in higher visual areas and virtually indistinguishable in V4 (Fig. 3B-E, blue curves). It appeared as if the representation of the suppressed orientation gradually receded along the ventral visual pathway, meanwhile the dominant orientation progressively took possession of all the available resources needed for neural representation. To measure the representational advantage of the dominant orientation over the suppressed orientation, we computed the suppression index (SI) (Wunderlich et al. 2005) as the degree to which the representational strength of the dominant orientation during rivalry approximated that when it was physically presented alone (i.e. the replay condition) in each ROI. An SI value close to 1 indicated full inhibition of the representation of the suppressed orientation during rivalry as if it were not presented, whereas an SI value close to 0 indicated highly comparable, if not equal, representational strength of the two competing orientations. Notably, the channel response corresponding to the suppressed orientation in the rivalry condition could be numerically negative in case of strong inhibition effects, which could generate SI values that exceeded 1.

Consistent with our observation, there was a gradual increase in SI from V1 to higher visual areas (Fig. 5A, one-way repeated measure ANOVA, $F_{(4, 36)} = 7.442$, $P < 0.001$).

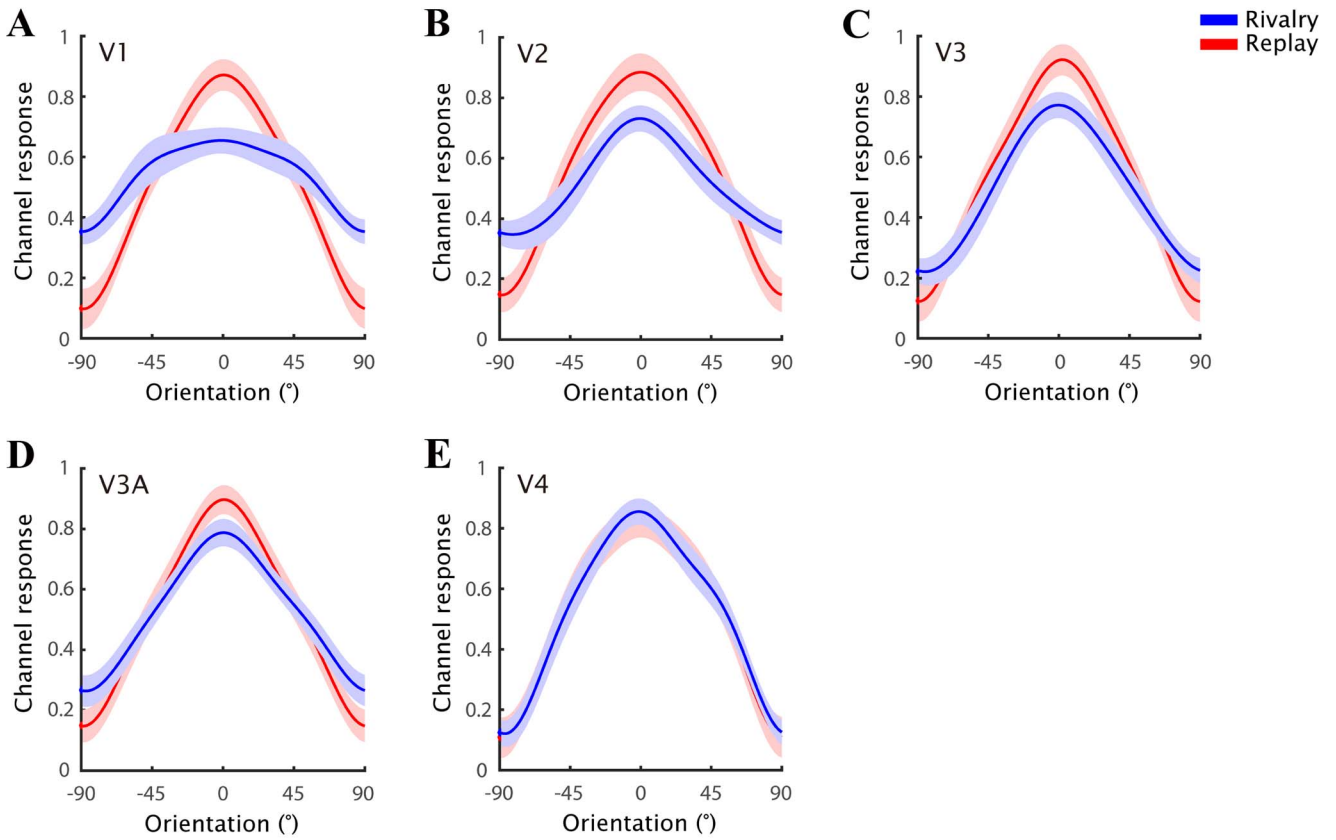

Fig. 3. A-E) Reconstructed channel response functions for the rivalry (blue) and the replay condition (red) in the orientation rivalry experiment. Shaded areas denote one S.E.M. across subjects.

This effect was further evaluated in two complementary ways. First, we explicitly tested for the inter-regional differences in SI using a non-parametric bootstrapping method. Specifically, we iteratively (10,000 times) resampled the subjects' SI data with replacement and calculated the averaged difference between two paired brain regions based on the resampled data in each iteration. We then obtained the distribution of the resampled SI differences. We found that SI increased from V1 to V4 (non-parametric bootstrapping method: V1 < V3: $P = 0.008$, V2 < V3: $P < 0.05$, V3 < V4: $P = 0.002$, V3A < V4: $P = 0.001$, 95% confidence interval (C.I.): V3-V1: [0.04, 0.49], V3-V2: [−0.02, 0.47], V4-V3: [0.12, 0.66], V4-V3A: [0.14, 0.67]), which further confirmed our observation. Second, we assessed whether the representation of the suppressed orientation was fully inhibited in each visual area during binocular rivalry by comparing its SI value against the value of 1 with bootstrapping. As a result, the maximal SI value was found in V4 with no significant difference from 1 ($P = 0.78$, 95% C.I.: [0.89,1.35]), while SIs of all the upstream cortical areas of V4 significantly deviated from full inhibition (V1: $P < 10^{-4}$, V2: $P < 10^{-4}$, V3: $P = 0.0041$, V3A: $P < 10^{-4}$, 95% C.I.: V1: [0.3, 0.6], V2: [0.36, 0.64], V3: [0.56, 0.92], V3A: [0.54, 0.85]). These findings were indicative of a continuous cortical transition from the co-existing neural representations of the rivalrous orientations in V1 to the dictatorial representation of the dominant orientation in V4, during which the suppressed orientation representation gradually diminished and eventually became fully inhibited. Importantly, the SI value was higher in V4 than that in V3A ($P = 0.0015$), suggesting that the suppressed orientation representation was "leaked out" rather than completely inhibited in V3A. Because V3A and V4 are located at the same level of the dorsal and ventral visual pathways, respectively, the contrast between partial versus full inhibition thus raised the possibility of different cortical evolutionary patterns of the rivalrous orientation representations in the two visual pathways during binocular rivalry.

Motion direction rivalry

Although our findings from the orientation rivalry experiment were suggestive of different neural dynamics associated with binocular rivalry between the ventral and the dorsal visual pathways, another possible explanation of the difference between V3A and V4 is that dorsal visual areas are not optimally engaged by orientation information processing, which might compromise the representational advantage of the dominant orientation in V3A. Furthermore, it remains unknown whether the cortical transition of the representations of rivalrous stimuli is contingent on stimulus type. To address these

issues, we conducted a second experiment to investigate the binocular rivalry between visual motions, a fundamental visual feature that have been shown to strongly drive dorsal visual areas (He et al. 1998; Fang and He 2005). We reasoned that, if the absence of full inhibition of the suppressed orientation in V3A could not be explained by the suboptimal stimulation of dorsal visual areas, then a similar cortical transition of rivalrous visual motion representations should be observed in the dorsal pathway akin to that of rivalrous orientation representations. The procedure and the design of the motion rivalry experiment were similar to those of the orientation rivalry experiment with three major modifications. First, in the main sessions, the monocular stimuli were replaced by two random dot kinetograms (RDK) moving in opposite directions that filled the same annular aperture. Second, in the localizer session, area MT+ was also identified in addition to areas V1-V4 and V3A due to its critical involvement in motion processing. Third, in the model training session, we modeled BOLD signal response to a motion direction as a linear combination of eight motion direction channel responses to provide a better coverage of the full span of possible motion directions. We employed the same data analysis pipeline to reconstruct and analyze the channel response functions in the motion direction rivalry experiment in those visual areas. Notably, 0° corresponded to the perceived and the viewed motion direction in the rivalry and the replay condition, respectively. Following the same logic as in the orientation rivalry experiment, response of the ±180° channel in the replay condition (i.e. the motion direction opposite to the viewed RDK) was used as the baseline.

Similar to the orientation rivalry experiment, we started by validating that the neural representations of the perceived and the viewed motion direction could be read out via the IEM. Behaviorally, the dominance duration distributions of the left-eye and the right-eye RDKs commonly conformed to a gamma distribution with no significant difference between the two eyes (Fig. 2B; mean duration of left eye RDK: 3.69 s, mean duration of right eye RDK: 3.90 s, Wilcoxon signed rank test: $P = 0.14$). At the neural level, a bell-shaped profile of the channel response function with a significant 0° peak in comparison to the baseline (i.e. the ±180° channel in the replay condition) was commonly identified in all the visual areas (Fig. 4, red curves, paired-t test: V1: $t_{(9)} = 14.237$, V2: $t_{(9)} = 18.380$, V3: $t_{(9)} = 11.153$, V3A: $t_{(9)} = 13.731$, MT+: $t_{(9)} = 15.294$, V4: $t_{(9)} = 11.366$, all $ps < 0.001$) in the replay condition. Moreover, we found that the 0° channel response in the rivalry condition was also significantly stronger than the baseline (Fig. 4, blue curves, paired-t test: V1: $t_{(9)} = 8.709$, V2: $t_{(9)} = 17.416$, V3: $t_{(9)} = 13.961$, V3A: $t_{(9)} = 8.210$, V4: $t_{(9)} = 13.898$, MT+: $t_{(9)} = 12.471$, all $ps < 0.001$). These results indicated that information of the perceived and the viewed motion directions could be extracted by our IEM approach, which further demonstrated the robustness of our approach.

Building on these results, we then investigated the neural representations of the rivalrous motion stimuli in the visual cortical areas. We made two observations that were highly consistent with the results of the orientation rivalry experiment. The first observation was the representation of the suppressed motion direction in V1, as reflected by the stronger ±180° channel response (i.e. the suppressed motion direction) in the rivalry condition than the baseline (Fig. 4A, $t_{(9)} = 5.237$, $P < 0.001$). The second was the representational advantage of the dominant motion stimulus in both visual pathways, as reflected by the stronger 0° channel response in comparison to the ±180° channel response (Fig. 4B-F, V1: $t_{(9)} = 4.331$, V2: $t_{(9)} = 10.067$, V3: $t_{(9)} = 16.152$, V3A: $t_{(9)} = 12.682$, MT+: $t_{(9)} = 11.355$, V4: $t_{(9)} = 13.545$, all $ps < 0.005$). Most importantly, while the representation of the suppressed motion direction was completely untraceable in the ventral area V4 (Fig. 4E) as the suppressed orientation representation, it nonetheless persisted in dorsal areas V3A and MT+ (Fig. 4D and F).

To quantify this effect, we computed the suppression index of motion direction rivalry and identified a similar graded pattern of suppression index across different visual areas as in the orientation rivalry experiment (Fig. 5B, one-way repeated-measure ANOVA, $F_{(5, 45)} = 3.045$, $P = 0.019$). This finding revealed a continuous attenuation of the suppressed motion direction representation accompanied by a simultaneous enhancement of the dominant motion direction representation. We performed the same statistical analyses to examine the inter-regional difference in SI and the degree of inhibition of the suppressed eye's motion direction. Similar to the orientation rivalry experiment, we found that SI gradually increased along the visual hierarchy (non-parametric bootstrapping: V1 < V2: $P < 0.001$, V1 < V3A: $P = 0.006$, V3A < V4: $P = 0.001$, 95% C.I.: V2-V1: [0.11, 0.57], V3A-V1: [0.06, 0.46], V4-V3A: [0.06, 0.33]). Importantly, the SI value of V4 exceeded not only that of V3A but also of MT+ ($P = 0.008$, 95% C.I.: V4-MT+: [0.03, 0.31]), which provided further evidence of full inhibition in the ventral but not in the dorsal visual areas. In contrast, however, there was no significant increase in suppression index from V3A to MT+ ($P = 0.46$, 95% C.I.: V3A-MT+: [−0.21, 0.16]). It appeared as if the "leaking" of the suppressed information continued along the dorsal pathway. Furthermore, only the SI in V4 was statistically indistinguishable from full inhibition ($P = 0.16$, 95% C.I.: [0.79, 1.06]), while SIs in all the other regions were significantly smaller than 1 (V1: $P < 10^{-4}$, V2: $P = 0.029$, V3: $P = 0.029$, V3A: $P < 10^{-4}$, MT+: $P = 0.001$, 95% C.I.: V1: [0.26, 0.71], V2: [0.61, 1.01], V3: [0.67, 1.00], V3A: [0.64, 0.82], MT+: [0.62, 0.91]). Together with the orientation rivalry experiment results, these findings advocated a progressive transition from co-existing representations of rivalrous stimuli to the dictatorial representation of the dominant stimulus that first emerged in V4. However, full inhibition of the suppressed stimulus was not observed in the dorsal areas.

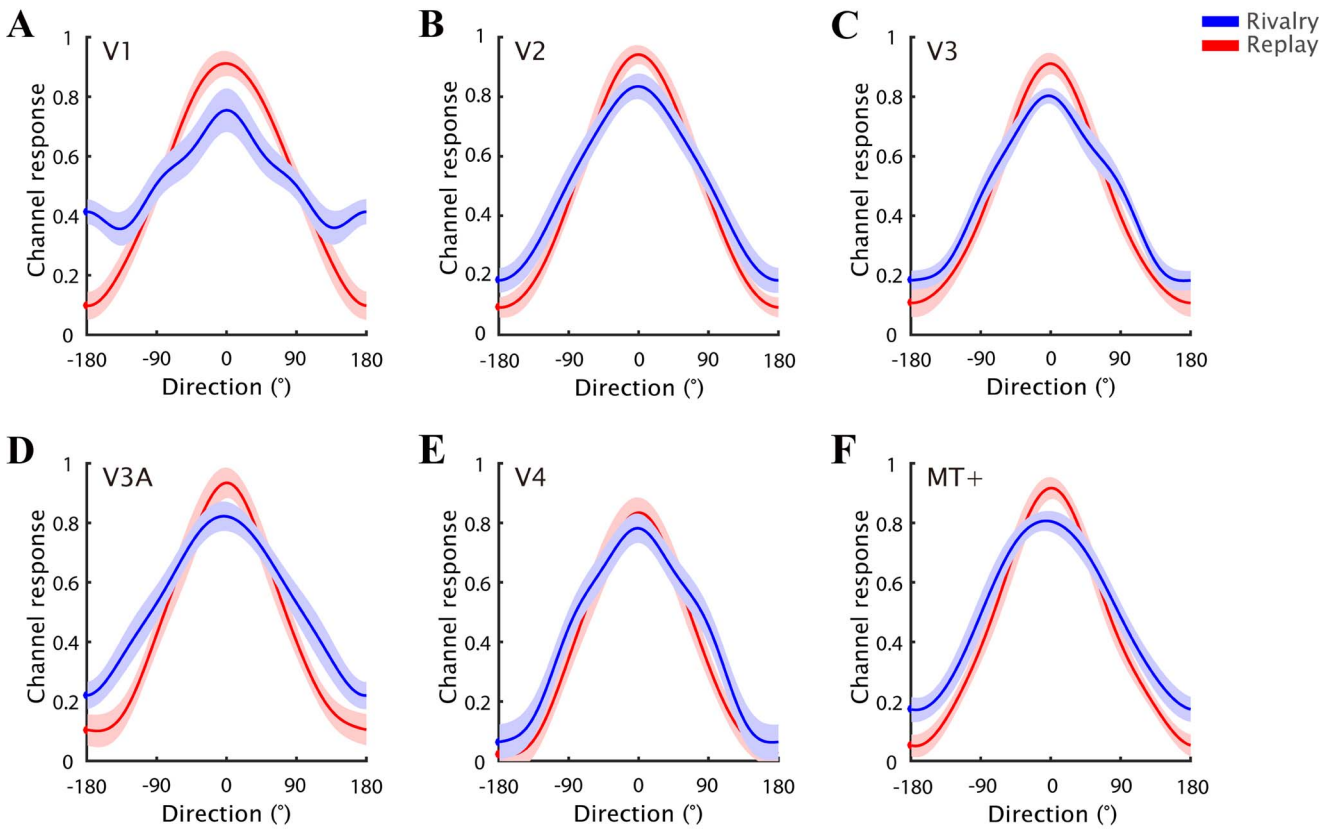

Fig. 4. A-F) Reconstructed channel response functions for the rivalry (blue) and the replay condition (red) in the motion direction rivalry experiment. Shaded areas denote one S.E.M. across subjects.

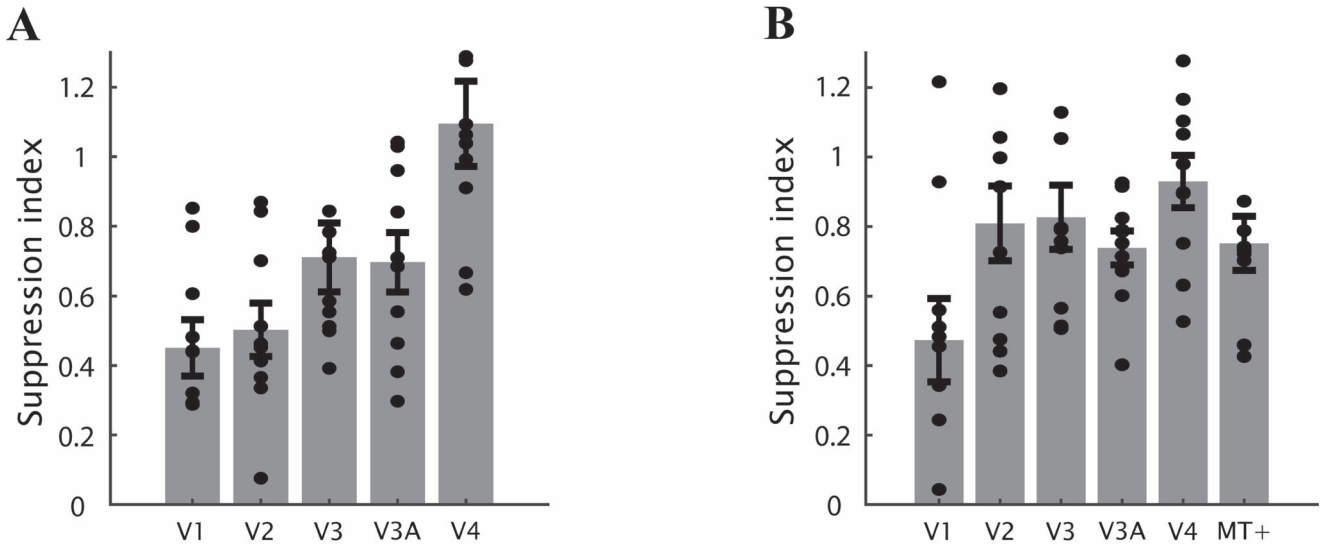

Fig. 5. Competitive advantage of the dominant stimulus representation over the suppressed stimulus representation quantified by suppression index in **A)** the orientation rivalry experiment and **B)** the motion direction rivalry experiment. Each dot denotes the data from a single subject. Error bars denote one S.E.M. across subjects.

Discussion

Using fMRI-based inverted encoding model analyses, we systematically investigated the neural representations of the rivalrous visual stimuli (i.e. orientations and motion directions) during binocular rivalry. We found that neural representations of the dominant and the suppressed stimuli co-existed in V1 with the dominant stimulus more strongly represented. Moreover, we further identified a gradual attenuation of the suppressed stimulus representation that was accompanied by a simultaneous

enhancement of the dominant representation. Notably, inhibition of the suppressed stimulus representation was fully completed in the ventral area V4, yet only partially completed in the dorsal areas located at the same and an even higher level of the visual processing hierarchy (i.e. V3A and MT+). Together, these findings revealed, for the first time, a progressive transition from the co-existing representations of the two eye's inputs to the dictatorial representation of the dominant eye's input from V1 to V4, suggesting a shift from interocular rivalry in early visual cortex to pattern rivalry in higher-order visual cortex.

Our findings provided two important insights concerning how retinal inputs are related to the perceptual content in the visual system, which were also corroborated by previous studies. First, our IEM approach revealed the population-level representations that signaled observers' perceptual status during binocular rivalry in visual areas as early as V1. This finding is consistent with previous fMRI studies on binocular rivalry (Polonsky et al. 2000; Tong and Engel 2001; Haynes et al. 2005; Lee et al. 2005; Wunderlich et al. 2005; Lee et al. 2007) and further confirms that the rivalry-induced perceptual alternations emerge from neural activities in early visual areas with minimal engagement of top-down consciousness-related feedbacks (Brascamp et al. 2015; Xu et al. 2016; Zou et al. 2016). Moreover, the weak yet robust representation of the suppressed stimulus in V1 is reminiscent of the evidence that information of invisible retinal stimuli is also encoded by neural activities in V1 (He et al. 1996; He and MacLeod 2001; Clifford and Harris 2005; Haynes and Rees 2005; Zhang et al. 2012). The present findings thus reinforce the pivotal role of V1 as the host of veridical representation of retinal inputs, even when they failed to gain access to visual awareness. Second, we identified a progressive magnification of the representational advantage of the dominant over the suppressed stimulus from V1 to higher-order extrastriate visual areas. Specifically, the population-level neural activation patterns in V4 were dictated by the dominant stimulus as if it was physically presented alone while there was no trace of the suppressed stimulus. This finding showed that the number of V4 neurons that tracked perceptual fluctuations might be more prevalent than what was previously identified (Leopold and Logothetis 1996), suggesting that higher-order extrastriate regions might serve as a proxy for the perceptual rather than the retinal contents of visual stimuli (Tong et al. 1998). In support of this idea, more recent findings showed that perceptual changes in binocular rivalry are initiated by a gradual accumulation of the neural activities associated with the impending changes across the visual hierarchy, which in turn leads to a top-down cascade of neural signals from higher-order to early visual areas that stabilizes the emerging percept (de Jong et al. 2020; Weilnhammer et al. 2021). Moreover, computational modeling results further demonstrated that the perceptual dynamics of binocular rivalry could be reproduced by a hierarchical model operating out of equilibrium (Cao et al 2021). Taken together, our findings argue against the idea that binocular rivalry is mediated by a single visual processing stage, but speak in favor of a comprehensive, multi-stage process involving a cascade of visual areas (Pearson and Clifford 2005).

So what might be the underlying neural mechanism that enables such representational transition process? In V1, monocular neurons are functionally organized into columnar structure (ocular dominance columns), making it an ideal host for the monocular input projected from eye-specific layers in lateral geniculate nuclei (LGN) via cortico-geniculate pathway (Ling et al. 2015). When the perceptually incompatible monocular signals arrived in V1, they trigger inhibitory interactions between the neuronal populations that are sensitive to the visual stimulus in each eye (i.e. interocular rivalry), thus leading to the co-existing representations that differed in strength. As the two eyes' inputs converge and travel to downstream visual areas, information of the competing monocular images is propagated to binocular neurons that are tuned to the respective visual feature patterns embedded in the two eyes' inputs, from which stage binocular rivalry proceeds in the form of competition between pattern-selective binocular neurons (i.e. pattern rivalry). Since neurons in higher-order visual areas are more susceptible to top-down feedback and exhibit more complex interaction (Zhang et al. 2011; Sprague and Serences 2013; Wang et al. 2013; Mo et al. 2018; Ge et al. 2020), the coupling between the conscious perceptual state and the neural representational dynamics is strengthened along the visual pathway, leading to increasingly stronger representation of the dominant stimulus and attenuated representation of the suppressed stimulus. Notably, the pattern rivalry effect is maximized when visual information arrived in V4 where neurons are selective to complex visual patterns (Okazawa et al. 2015; Ziemba and Freeman 2015; Kim et al. 2019). Our findings thus suggest that the two seemingly distinctive neural mechanisms of binocular rivalry postulated in previous studies, namely interocular rivalry and pattern rivalry, might essentially be two consecutive stages of a unified process.

However, our findings raised a critical question concerning the ambiguous involvement of dorsal visual areas in binocular rivalry. On one hand, representation of the suppressed stimulus was attenuated in both dorsal and ventral visual areas. On the other hand, whereas information of the invisible monocular stimulus was discarded in the ventral area V4, it appeared to be retained, albeit to a small degree, in the dorsal areas of the same or a higher level in the visual system. Moreover, this "leaking" effect could not be explained by the difference in cortical sensitivity to stimulus features. These findings thus suggest that representations of the rivalrous monocular stimuli might go through different cortical transition processes in the two pathways that are differed in the source of their inputs. For the cortical routes, it has been shown that dorsal and ventral

regions are primarily driven by input signals initially from the magnocellular and the parvocellular pathways, respectively (Goodale and Milner 1992; Poltoratski et al. 2019), and the latter is more heavily involved in binocular rivalry (He et al. 2005). Moreover, motion-sensitive dorsal visual areas, such as MT+, might also receive inputs projected directly from LGN via a pathway that bypass the canonical cortical routes (Sincich et al. 2004). As a result of the combined contributions of these two factors, representation of the suppressed stimulus was able to survive in the dorsal areas despite increasingly stronger inhibition effects along both the ventral and dorsal visual pathways. In line with this idea, previous human fMRI findings showed that BOLD signals in ventral visual areas decreased when the visual stimuli were rendered invisible via interocular suppression (Fang and He 2005) or motion induced blindness (Donner et al. 2008), while neural activities in the dorsal visual areas were less influenced by observers' conscious perception. Although reduced dorsal activity for invisible visual objects was observed in several previous studies (Hesselmann and Malach 2011; Hesselmann et al. 2018), these observations could be explained by the way in which the suppressed stimuli were rendered subjectively invisible (Fogelson et al. 2014). In those studies, a temporally dynamic, high-contrast Mondrian mask was presented to one eye, which might introduce additional noise that further weakened the dorsal activities related to the high-level features of the suppressed eye's image (Almeida et al. 2008; Almeida et al. 2010). The dorsal and ventral pathways might thus play different roles in binocular rivalry and other perceptual processes in which perceptual experience and retinal inputs are dissociated.

Although it is tempting to interpret the dictatorial representation of the dominant stimulus in V4 as the evidence that binocular rivalry is resolved in this region, extreme cautions should be taken when attempting to draw such a conclusion. First, due to the spatial coverage limitation of our imaging data, we were unable to investigate the neural representations in cortical areas beyond V4. It is therefore difficult to ascertain whether the neural signals in V4 resulted from local neuronal processing within this region or top-down feedbacks from higher-order cortical regions. In the latter case, it is possible that binocular rivalry is resolved in fronto-parietal regions, rather than V4. It has been shown that complex cognitive functions typically mediated in fronto-parietal regions, such as attention and action planning, might be involved in various aspects of bi-stable perception (Sterzer et al. 2009; Knapen et al. 2011; Brascamp et al. 2018). In line with this idea, it was recently proposed that inferior frontal cortex is causally involved in determining the contents of conscious experience, as disruption of neural activity in this area hinders the alternation of percepts (Weilnhammer et al. 2021). Second, the channel response functions reconstructed by the IEM reflect only the population-level neural dynamics from aggregated measurements (Sprague et al. 2018). With the limited spatial and temporal resolution of fMRI data, characterizing the neuronal interaction that accomplishes full inhibition of the suppressed stimulus is highly challenging. Future research efforts are still needed to fully elucidate the neural correlates of binocular rivalry.

In summary, our findings provide novel and systematic experimental evidence that reconciles previous discrepant findings concerning the mechanisms of binocular rivalry. We show that binocular rivalry is not mediated by a single stage of visual cortical processing, but rather recruit multiple processing stages. These findings invite us to rethink how consciousness is related to the neural dynamics in multiple interacting brain regions that span different levels of the cortical system.

Funding

This study was supported by the National Science and Technology Innovation 2030 Major Program 2022ZD0204802, the National Natural Science Foundation of China (31930053, 32000379) and Beijing Academy of Artificial Intelligence (BAAI).

Conflict of interest statement: The authors declare no conflicts of interest.

References

Alais D, Blake R. *Binocular rivalry*. MIT press, Cambridge, Massachusetts, MA 02142.

Almeida J, Mahon BZ, Nakayama K, Caramazza A. Unconscious processing dissociates along categorical lines. *Proc Natl Acad Sci*. 2008:105:15214–15218.

Almeida J, Mahon BZ, Caramazza A. The role of the dorsal visual processing stream in tool identification. *Psychol Sci*. 2010:21:772–778.

Blake R. A primer on binocular rivalry, including current controversies. *Brain and Mind*. 2001:2:5–38.

Blake R, Logothetis NK. Visual competition. *Nat Rev Neurosci*. 2002:3:13–21.

Blake R, Brascamp J, Heeger DJ. Can binocular rivalry reveal neural correlates of consciousness? *Philos Trans R Soc Lond Ser B Biol Sci*. 2014:369:20130211.

Brascamp J, Blake R, Knapen T. Negligible fronto-parietal BOLD activity accompanying unreportable switches in bistable perception. *Nat Neurosci*. 2015:18:1672–1678.

Brascamp J, Sterzer P, Blake R, Knapen T. Multistable perception and the role of the frontoparietal cortex in perceptual inference. *Annu Rev Psychol*. 2018:69:77–103.

Brouwer GJ, Heeger DJ. Decoding and reconstructing color from responses in human visual cortex. *J Neurosci*. 2009:29:13992–14003.

Brouwer GJ, Heeger DJ. Categorical clustering of the neural representation of color. *J Neurosci*. 2013:33:15454–15465.

Cao R, Pastukhov A, Aleshin S, Mattia M, Braun J. Binocular rivalry reveals an out-of-equilibrium neural dynamics suited for decision-making. *elife*. 2021:10:e61581.

Clifford CW. Binocular rivalry. *Curr Biol*. 2009:19:R1022–R1023.

Clifford CW, Harris JA. Contextual modulation outside of awareness. *Curr Biol*. 2005:15:574–578.

DiCarlo JJ, Zoccolan D, Rust NC. How does the brain solve visual object recognition? *Neuron*. 2012:73:415–434.

Donner TH, Sagi D, Bonneh YS, Heeger DJ. Opposite neural signatures of motion-induced blindness in human dorsal and ventral visual cortex. *J Neurosci*. 2008:28:10298–10310.

Ester EF, Sprague TC, Serences JT. Parietal and frontal cortex encode stimulus-specific mnemonic representations during visual working memory. *Neuron*. 2015:87:893–905.

Fang F, He S. Cortical responses to invisible objects in the human dorsal and ventral pathways. *Nat Neurosci*. 2005:8:1380–1385.

Fogelson SV, Kohler PJ, Miller KJ, Granger R, Tse PU. Unconscious neural processing differs with method used to render stimuli invisible. *Front Psychol*. 2014:5:601.

Ge Y, Zhou H, Qian C, Zhang P, Wang L, He S. Adaptation to feedback representation of illusory orientation produced from flash grab effect. *Nat Commun*. 2020:11:3925.

Goodale MA, Milner AD. Separate visual pathways for perception and action. *Trends Neurosci*. 1992:15:20–25.

Haynes JD, Rees G. Predicting the orientation of invisible stimuli from activity in human primary visual cortex. *Nat Neurosci*. 2005:8:686–691.

Haynes J-D, Rees G. Decoding mental states from brain activity in humans. *Nat Rev Neurosci*. 2006:7:523–534.

Haynes J-D, Deichmann R, Rees G. Eye-specific effects of binocular rivalry in the human lateral geniculate nucleus. *Nature*. 2005:438:496–499.

He S, MacLeod DI. Orientation-selective adaptation and tilt aftereffect from invisible patterns. *Nature*. 2001:411:473–476.

He S, Cavanagh P, Intriligator J. Attentional resolution and the locus of visual awareness. *Nature*. 1996:383:334–337.

He S, Cohen ER, Hu X. Close correlation between activity in brain area MT/V5 and the perception of a visual motion aftereffect. *Curr Biol*. 1998:8:1215–1218.

He S, Carlson T, Chen X. *Parallel pathways and temporal dynamics in binocular rivalry*; MIT press 2005.

Hesselmann G, Malach R. The link between fMRI-BOLD activation and perceptual awareness is "stream-invariant" in the human visual system. *Cereb Cortex*. 2011:21:2829–2837.

Hesselmann G, Darcy N, Rothkirch M, Sterzer P. Investigating masked priming along the "vision-for-perception" and "vision-for-action" dimensions of unconscious processing. *J Exp Psychol Gen*. 2018:147:1641.

de Jong MC, Vansteensel MJ, van Ee R, Leijten FSS, Ramsey NF, Dijkerman HC, Dumoulin SO, Knapen THJ. Intracranial recordings reveal unique shape and timing of responses in human visual cortex during illusory visual events. *Curr Biol*. 2020:30:3089–3100.e4.

Kamitani Y, Tong F. Decoding the visual and subjective contents of the human brain. *Nat Neurosci*. 2005:8:679–685.

Kim T, Bair W, Pasupathy A. Neural coding for shape and texture in macaque area V4. *J Neurosci*. 2019:39:4760–4774.

Kleiner M, Brainard D, Pelli D, Ingling A, Murray R, Broussard C. What's new in Psychtoolbox-3? *Perception*. 2007:36:1–16.

Knapen T, Brascamp J, Pearson J, van Ee R, Blake R. The role of frontal and parietal brain areas in bistable perception. *J Neurosci*. 2011:31:10293–10301.

Lee SH, Blake R, Heeger DJ. Traveling waves of activity in primary visual cortex during binocular rivalry. *Nat Neurosci*. 2005:8:22–23.

Lee SH, Blake R, Heeger DJ. Hierarchy of cortical responses underlying binocular rivalry. *Nat Neurosci*. 2007:10:1048–1054.

Leopold DA, Logothetis NK. Activity changes in early visual cortex reflect monkeys' percepts during binocular rivalry. *Nature*. 1996:379:549–553.

Ling S, Pratte MS, Tong F. Attention alters orientation processing in the human lateral geniculate nucleus. *Nat Neurosci*. 2015:18:496–498.

Logothetis NK, Schall JD. Neuronal correlates of subjective visual perception. *Science*. 1989:245:761–763.

Logothetis NK, Leopold DA, Sheinberg DL. What is rivalling during binocular rivalry? *Nature*. 1996:380:621–624.

Mishkin M, Ungerleider LG, Macko KA. Object vision and spatial vision: two cortical pathways. *Trends Neurosci*. 1983:6:414–417.

Mo C, He D, Fang F. Attention priority map of face images in human early visual cortex. *J Neurosci*. 2018:38:149–157.

Mo C, Lu J, Wu B, Jia J, Luo H, Fang F. Competing rhythmic neural representations of orientations during concurrent attention to multiple orientation features. *Nat Commun*. 2019:10:5264.

Okazawa G, Tajima S, Komatsu H. Image statistics underlying natural texture selectivity of neurons in macaque V4. *Proc Natl Acad Sci*. 2015:112:E351–E360.

Pearson J, Clifford CW. Suppressed patterns alter vision during binocular rivalry. *Curr Biol*. 2005:15:2142–2148.

Polonsky A, Blake R, Braun J, Heeger DJ. Neuronal activity in human primary visual cortex correlates with perception during binocular rivalry. *Nat Neurosci*. 2000:3:1153–1159.

Poltoratski S, Maier A, Newton AT, Tong F. Figure-ground modulation in the human lateral geniculate nucleus is distinguishable from top-down attention. *Curr Biol*. 2019:29:2051–2057.e3.

Rademaker RL, Chunharas C, Serences JT. Coexisting representations of sensory and mnemonic information in human visual cortex. *Nat Neurosci*. 2019:22:1336–1344.

Schurger A. A very inexpensive MRI-compatible method for dichoptic visual stimulation. *J Neurosci Methods*. 2009:177:199–202.

Sheinberg DL, Logothetis NK. The role of temporal cortical areas in perceptual organization. *Proc Natl Acad Sci*. 1997:94:3408–3413.

Sincich LC, Park KF, Wohlgemuth MJ, Horton JC. Bypassing V1: a direct geniculate input to area MT. *Nat Neurosci*. 2004:7:1123–1128.

Sprague TC, Serences JT. Attention modulates spatial priority maps in the human occipital, parietal and frontal cortices. *Nat Neurosci*. 2013:16:1879–1887.

Sprague TC, Ester EF, Serences JT. Restoring latent visual working memory representations in human cortex. *Neuron*. 2016:91:694–707.

Sprague TC, Adam KCS, Foster JJ, Rahmati M, Sutterer DW, Vo VA. Inverted encoding models assay population-level stimulus representations, not single-unit neural tuning. *eNeuro*. 2018:5:ENEURO.0098–0018.2018.

Sterzer P, Kleinschmidt A, Rees G. The neural bases of multistable perception. *Trends Cogn Sci*. 2009:13:310–318.

Tong F. Competing theories of binocular rivalry: a possible resolution. *Brain and Mind*. 2001:2:55–83.

Tong F, Engel SA. Interocular rivalry revealed in the human cortical blind-spot representation. *Nature*. 2001:411:195–199.

Tong F, Nakayama K, Vaughan JT, Kanwisher N. Binocular rivalry and visual awareness in human extrastriate cortex. *Neuron*. 1998:21:753–759.

Tong F, Meng M, Blake R. Neural bases of binocular rivalry. *Trends Cogn Sci*. 2006:10:502–511.

Wang M, Arteaga D, He BJ. Brain mechanisms for simple perception and bistable perception. *Proc Natl Acad Sci*. 2013:110:E3350–E3359.

Watson TL, Pearson J, Clifford CW. Perceptual grouping of biological motion promotes binocular rivalry. *Curr Biol*. 2004:14:1670–1674.

Weilnhammer VA, Fritsch M, Chikermane M, Eckert ALL, Kanthak K, Stuke H, Kaminski J, Sterzer P. An active role of inferior frontal cortex in conscious experience. *Curr Biol*. 2021:31:2868–2880.e8.

Wunderlich K, Schneider KA, Kastner S. Neural correlates of binocular rivalry in the human lateral geniculate nucleus. *Nat Neurosci*. 2005:8:1595–1602.

Xu H, Han C, Chen M, Li P, Zhu S, Fang Y, Hu J, Ma H, Lu HD. Rivalry-like neural activity in primary visual cortex in anesthetized monkeys. *J Neurosci*. 2016:36:3231–3242.

Zhang P, Jamison K, Engel S, He B, He S. Binocular rivalry requires visual attention. *Neuron*. 2011:71:362–369.

Zhang X, Zhaoping L, Zhou T, Fang F. Neural activities in V1 create a bottom-up saliency map. *Neuron*. 2012:73:183–192.

Ziemba CM, Freeman J. Representing "stuff" in visual cortex. *Proc Natl Acad Sci*. 2015:112:942–943.

Zou J, He S, Zhang P. Binocular rivalry from invisible patterns. *Proc Natl Acad Sci*. 2016:113:8408–8413.